Hindawi
Geofluids
Volume 2019, Article ID 9874168, 17 pages
https://doi.org/10.1155/2019/9874168

Research Article

Influence of Overlying Caprock on Coalbed Methane Migration in the Xutuan Coal Mine, Huaibei Coalfield, China: A Conceptional Analysis on Caprock Sealability

Kaizhong Zhang,[1,2,3] **Qingquan Liu**,[1,2,3] **Kan Jin**,[1,2,3,4] **Liang Wang**,[1,2,3] **Yuanping Cheng**,[1,2,3] **and Qingyi Tu**[1,2,3]

[1]*Key Laboratory of Gas and Fire Control for Coal Mines (China University of Mining and Technology), Ministry of Education, Xuzhou 221116, China*
[2]*National Engineering Research Center for Coal & Gas Control, China University of Mining and Technology, Xuzhou 221116, China*
[3]*School of Safety Engineering, China University of Mining and Technology, Xuzhou 221116, China*
[4]*College of Quality & Safety Engineering, China Jiliang University, Hangzhou, Zhejiang 310018, China*

Correspondence should be addressed to Liang Wang; liangw1982@126.com and Yuanping Cheng; cyp620924@outlook.com

Received 15 October 2018; Revised 8 January 2019; Accepted 5 February 2019; Published 9 April 2019

Academic Editor: Huazhou Li

In order to determine the controlling factors affecting coalbed gas migration in the Xutuan coal mine, Huaibei Coalfield, China, overlying caprocks with Quaternary and Neogene formation (loose bed), Paleogene formation (Redbed), and coal-bearing strata were investigated via petrography, lithology, and physical properties according to laboratory tests, theoretical analysis, and on-site exploration. Results indicate that the basic properties of coal were not significantly changed whereas the effect of coalbed gas escape was promoted in the presence of Redbed and loose bed. The pore structure analysis shows that Redbed has well-developed pore connectivity than coal-bearing strata (main components are sandstone, siltstone, and mudstone). Also, the diffusion coefficient and permeability of Redbed and loose bed are proved to be a little different than those of sandstone but are much higher than those of mudstone and siltstone. Based on the aforementioned findings, investigation on the sealing mechanism of overlying caprocks on CBM migration was further discussed, interpreting that the thickness, permeation, and diffusion features are crucial factors for sealing capacity of the overlying caprock. Thus, with the simplification on the thickness of overlying strata, a conceptional analysis was carried out to theoretically estimate the sealability of caprocks from surface drilling holes; it appears, though, that the master factor on coalbed methane accumulation is coal-bearing strata instead of Redbed and loose bed with a poor sealability. In this case, the reliability of the evaluation method could be indirectly validated from the on-site gas content data of the actual coal seam to fundamentally reflect the effect of Redbed and loose bed on gas-escaping, and the impact of coal-bearing strata on gas accumulation in the coal seam.

1. Introduction

As one of the most indispensable unconventional resources, methane in coal has attracted more and more attention from governments and scholars [1–3]. The production of methane from coal is derived from two ways: coal mine methane (CMM) and coalbed methane (CBM) [4]. Due to the complex geological conditions with controlling factors, commercial exploitation of CBM and CMM has experienced diverse geological hazards in developing countries, such as gas disasters in coal mine [5–7]. Therefore, considerable attention should be paid to the comprehensive methane control and utilization that are related to safety, economy, and environmental effects [8, 9]. Here, systematic knowledge of gas migration in coal seam is critical for the methane control and utilization project. Gas accumulation characteristics, which were heavily investigated in previous researches, are associated with geological evolution history, degree of

coalification, geological tectonism, depth of burial, permeability of surrounding rock, and hydrogeology [10–12]. From the perspective of gas geology, the residual gas content during a long-term geologic process (gas content) can be regarded as an effective indicator for gas accumulation characteristic, which depends on the reservoir condition of gas migration and storage capacity [13, 14].

In the field of CBM and CO_2-ECBM, previous studies were mostly focused on the sealing capacity of coal reservoir, CBM accumulation, and migration [14–17]. As the source rock, coal has the ability to transport and store CBM and may be affected by stratigraphic traps and structural traps, which are developed in coal-bearing strata [18, 19]. Stratigraphic traps are common in the coal-bearing strata that are mainly governed by sealing rocks, such as mudstone, siltstone, and sandstone, and their thickness controls the sealability [15], whereas structural traps are only generated from the fault-sealing strata, influenced by tectonic movement, sedimentary environment, and fault evolution [20, 21]. Investigation on the geological characteristic of CBM reservoirs may contribute to the commercial potential of CBM exploration [22]. Meanwhile, in the field of CO_2-ECBM, scholars prefer to study the behaviors and mechanism of caprock-sealing and their potential effects on CO_2 leakage pathways that are conducted as following topics: laboratory experiments, numerical simulation, and natural analogues [23–25]. For laboratory experiments, attention was paid to the basic parameter, microfracture, pore geometry, and microfabric of coal and rocks; however, it is limited to identify the in situ sealing capacity of caprock for a geological timescale [23]. Although numerical simulation may narrow the gap in this regard, the availability needs to be checked by field application [23, 24]. Natural analogues highlight verification of the numerical models estimating sealing capacity without sufficient basis on the theory [25–27]. Totally, the existing literatures on this subject cover the sealability mechanism of caprock with qualitative and quantitative studies in laboratory experiments, numerical simulation, and natural analogues [14]. However, conceptional descriptions on caprock sealability have insufficient support in field application. Thus, such evidence should be concerned with the geological factors related to actual coal seam to determine CBM migration and yield insights into the sealing properties of caprock.

Actually, studies on the geological factors affecting CBM migration are difficult to conduct due to the fact there exist complex factors affecting the sealing properties of caprock [28, 29]. Accidentally, it has been discovered that an actual geological unit of the Xutuan coal mine of Huaibei Coalfield in China has the particular lithological features of caprocks with Quaternary formation, Neogene formation, and Paleogene formation (Redbed) overlying the coal-bearing strata of the CBM reservoir; with little influence of tectonism, the studying area of the Xutuan coal mine is more suitable for exploring the sealing capacity of caprock [30]. On the one hand, previous studies indicated that Paleogene formation (Redbed), i.e., the clasolite continental deposit (composed of conglomerate and sandstone), presents certain discrepancies with coal-bearing strata and is widely distributed in China [31, 32]. Also, it has been revealed that the dissipation effect of Redbed on gas accumulation could be demonstrated by the comparison of the physical differences between Redbed and coal-bearing strata rocks [30]. On the other hand, the thickness of each stratum in caprock may promote the CBM accumulation and migration; thus, the factors affecting CBM migration may be determined by the lithology and thickness of caprocks [33]. Studies on the caprocks are crucial for understanding the sealing mechanism on gas migration and its controlling effect [33]. Unfortunately, scholars rarely focus on this topic, especially the comprehensive analysis of gas migration under the caprocks containing the Redbed, as well as a logical evaluation of sealability. In this case, an evaluation method for caprock sealability is theoretically discussed based on lithological properties and thickness of caprock.

This paper presents a comparative study on the physical parameters of the coal-bearing strata (sandstone, mudstone, and siltstone), Paleogene formation (Redbed), Neogene formation, and Quaternary formation via the petrography, lithology, pore structure, diffusion, and permeability. Combined with coalbed gas parameters in the field, a schematic description of CBM migration with a semiquantitative evaluation on the sealability of caprocks was proposed, which highlights the controlling factor affecting CBM migration in the Xutuan coal mine.

2. Geological Setting of the Study Area

The Linsu mining area, Huaibei Coalfield, is located between north of the Bengbu rise and south of the Subei fault belt in the EW direction and distributed in the graben structure area of Subei (NE-trending) and Guangwu-Guzhen (NE-trending) fault belts. As shown in Figure 1, the Linsu mining area has experienced many geological activities due to the complex geological tectonism. During the late indosinian movement, the collision of the North and South China plates weakened, leading to the stretched rift with EW-trending faults and folds such as Sunan syncline, Tongting anticline, Nanping syncline, and Subei fault [34, 35].

The Xutuan coal mine is located in the center of Huaibei Plain, adjacent to the Tongting anticline on the north and the Banqiao fault on the south. As shown in Figure 1, large folds and fractures of the Xutuan coal mine are less developed with a flat terrain except for some small faults sporadically distributed in the Linsu mining area. The whole study area is considered as having a stable condition without strong heterogeneity and tectonism influence, supplying the paleotopography and depositional settings for the Paleogene formation (Redbed). The primary mineable coal seam in the Xutuan coal mine is mining area 33, the southeast part of which deposited a large area of thick Redbed, as shown in Figure 1. The Redbed in the Xutuan coal mine, with an unconformity on coal-bearing strata, thickened gradually from the northwest to southeast direction. Earlier studies have proven that the influence of an inland subtropical arid climatic zone in the central region of China on rock weathering provides rich rock weathering for the formation of Redbed [36]. With high-temperature effect, sedimentary

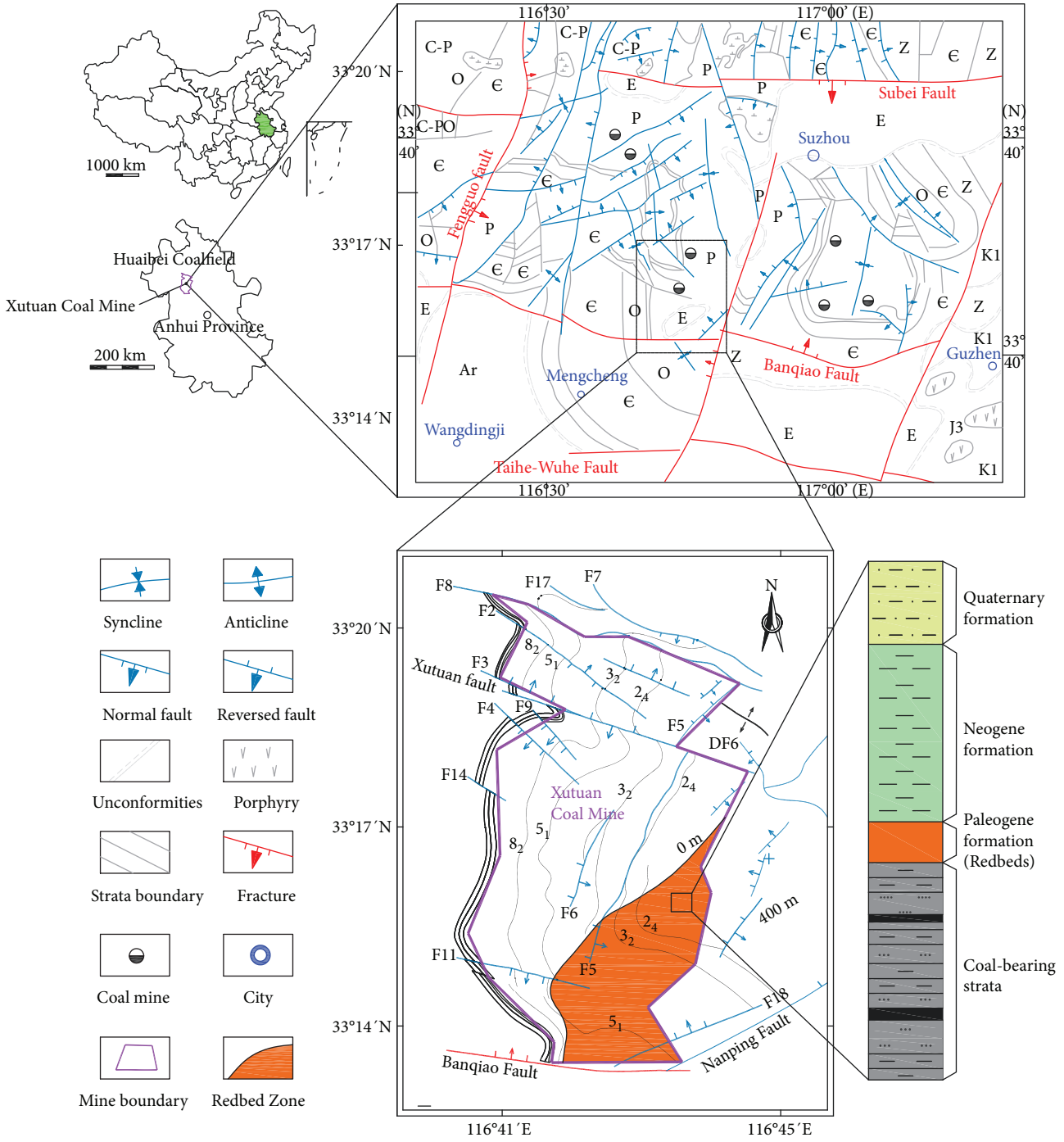

Figure 1: Regional structure of the Lin-Su mining area in Huaibei Coalfield and structural outlines of the Xutuan coal mine.

rock has experienced strong oxidation and gradually changed into red [37].

In mining area 33, the overlying caprock of the normal zone (which is not covered with Redbed) contains Quaternary formation, Neogene formation, and coal-bearing strata. And the overlying caprock of the Redbed zone contains Quaternary formation, Neogene formation, Paleogene formation (Redbed), and coal-bearing strata. The floor of mining area 33 is composed primarily of bauxitic mudstone in the Permian Lower Shihezi Formation, which acts as a barrier to gas transport and plays an important role in coalbed gas preservation.

3. Sampling and Methods

3.1. Sample Preparation. To study CBM accumulation in the Xutuan coal mine, the coal was sampled from the underground coal seam and its overlying caprocks were obtained through surface drilling holes. For the sampling in the underground of the coal seam, coal samples in the normal and

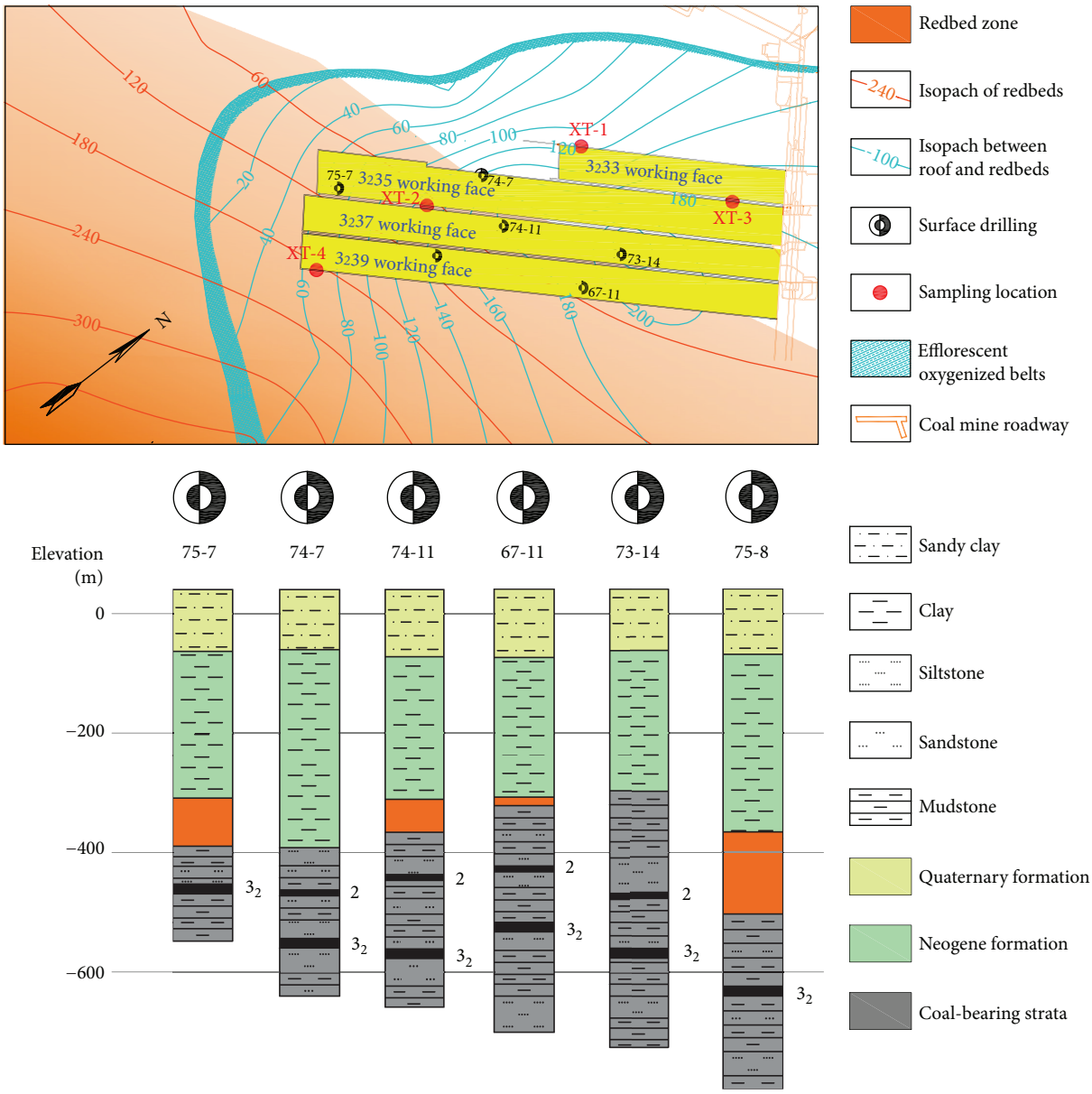

Figure 2: Distribution map of sampling location.

Redbed zones were collected from a freshly exposed mining face, sealed, and sent to the laboratory without any delay to prevent oxidation. The underground sampling locations are shown in Figure 2. The coal samples were crushed and screened to the appropriate quantity and sizes according to the purpose, methods, and instrument of experiments.

The rock samples of overlying caprocks were obtained from surface drilling holes (75-7, 74-7, 74-11, 67-11, 73-14, and 75-8), the locations of which are presented in Figure 2. It can be explicitly inferred that the elevations of the surface drilling holes ranged from −480 m to −660 m; the surface drilling holes are almost distributed in the Redbed zone except 74-7. The isopach between roof and Redbed, i.e., the thickness of the coal-bearing strata, is gradually deeper from the W direction to the E direction, with the thickness order of 75-7 < 74-7 < 75-8 < 74-11 < 67-11 < 73-14.

From sampling sites of surface drilling, as shown in Figures 2 and 3, it can be recognized that the caprocks mainly contain Quaternary and Neogene formations (which are regarded as loose bed), Paleogene formation (Redbed), and coal-bearing strata. Coal-bearing strata are mainly composed of mudstone, siltstone, and sandstone. Rock samples were made into standard samples (cylindrical), the diameter and height of which are 50 mm and 100 mm, respectively, and were adopted to perform the diffusion and permeability tests.

3.2. Experimental Methods. According to China National Standard GB/T 212-2008 and GB/T 6948-2008, proximate and petrographic analyses of moisture, ash, and volatile matter and mean maximum reflectance of vitrinite with maceral proportion were conducted using the 55E-MAG6600 automatic proximate analyzer (Changsha Kaiyuan Instruments,

(a) Surface drilling in the field (b) The core of drilling hole

(c) The standard sample ($\varphi 50 \times 100$ mm) of caprocks

Figure 3: Field sampling process of caprocks and the standard sample preparation.

China) and microscope photometer (Zeiss, Germany), respectively. Following the Washburn equation, pore size distributions of coal and rock samples were characterized by mercury intrusion porosimetry (MIP) using an AutoPore IV 9500 mercury porosimeter (Micromeritics, USA), which can measure pore diameters of 3-100000 nm over a pressure range of 0.1-450 MPa [38]. Additionally, China National Standard GB/T 19560-2008 is regarded as guidance on adsorption constant through HCA high-pressure volumetric equipment (Chongqing Research Institute of CCTEG, China).

Diffusion property tests of rock samples were performed by the KDKX-II block coal diffusion coefficient analyzer (Nantong Kedi Instruments, China), as shown in Figure 4. Test procedures could be described as follows. Firstly, the cylindrical coal and rock samples of the surface drilling hole were loaded in the holder with a confining pressure range of 0.5-3 MPa and a constant temperature of 30°C. After evacuation for 24 h, methane pressure and helium pressure were maintained at the same gas pressure to avoid pressure-driven permeation. Next, the chromatographic analysis of the gases was conducted, and the diffusion coefficient was calculated through a counter diffusion method, which could be derived from the diffusion concentration difference between both ends of the sample container. Systematic knowledge about the counter diffusion method is shown in Section 4.2.3.

The permeability tests of samples were conducted through a homemade instrument (a triaxial multigas apparatus), as presented in Figure 5. The cylindrical sample was initially placed between two loading platens with the methane pressure difference between upstream and downstream of the sample. The loading module was used to adjust the sample with a confining pressure range of 2-15 MPa; the temperature transducer is adopted to maintain the fluid temperature to a constant temperature of 30°C. In this case, the pressure and flow rate are determined and controlled by an injection pump. The permeability tests of samples were performed through the fluid module according to the transient pressure method, which is detailedly introduced in Section 4.2.3.

4. Results and Analyses

4.1. Basic Properties of Coal Seam Effected by Redbed. The proximate analysis and adsorption constant of coal samples of the normal zone (XT-1, XT-3) and Redbed zone (XT-2, XT-4) are listed in Table 1. The moisture content of all coal samples was slightly changed around 1.1%, belonging to low moisture coal. The volatile matter was held at 20.6~23.17%, which may be determined as high volatile bituminous coal. In general, there is no obvious difference between these four coal samples, indicating that the presence of Redbed has little effect on the coal sample in mining area 33. For adsorption constant, the ranges of V_L and P_L are 23.88~24.47 m^3/t and 1.60~1.77 MPa, which are not impacted by the Redbed.

Petrography studies, as shown in Figure 6(a), reveal that vitrinite reflectance of coal samples XT-1 and XT-3 in the

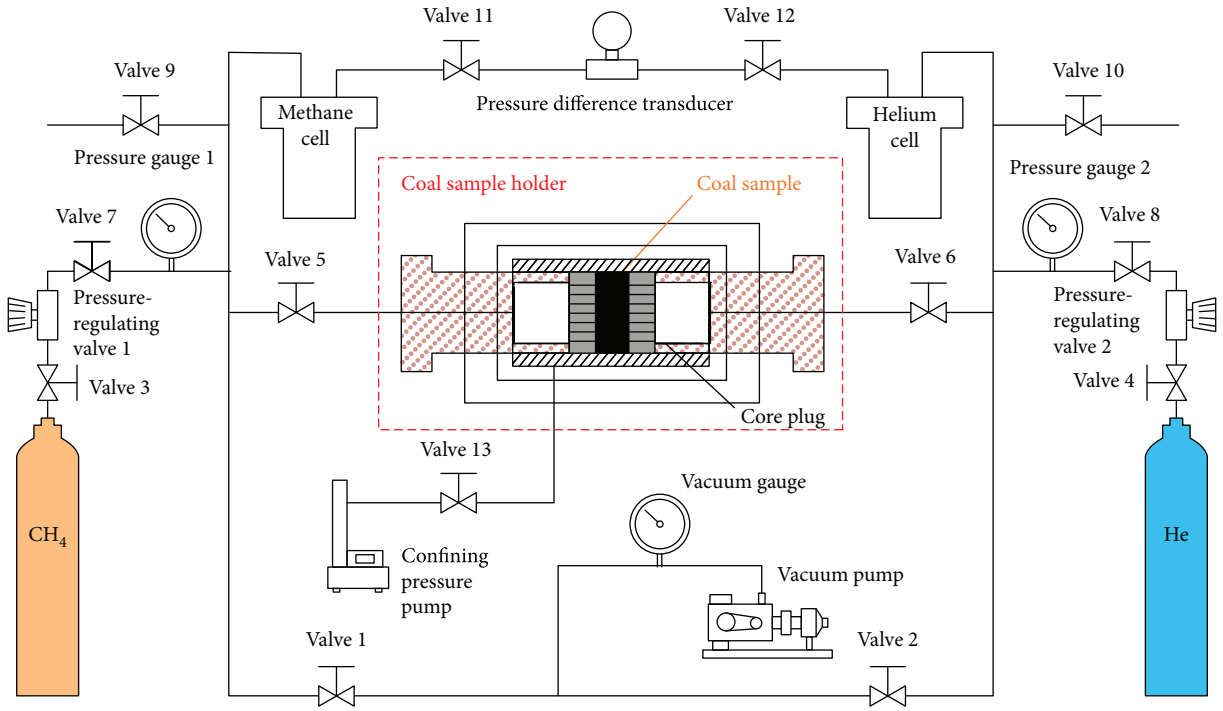

Figure 4: Schematic diagram of counterdiffusion experiment modified from Dong et al. [39].

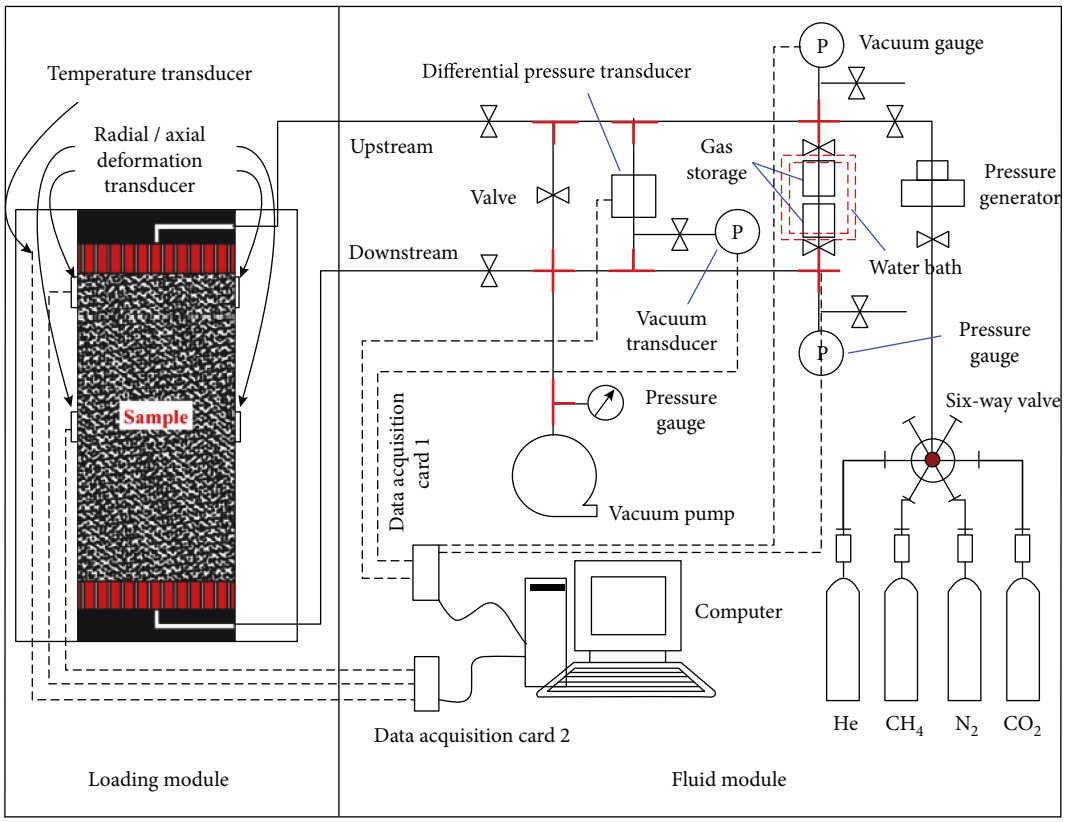

Figure 5: Schematic diagram of the experimental apparatus using the transient pressure method modified after Chen et al. [40].

normal zone and XT-2 and XT-4 in the red zone ranges from 0.78% to 0.89%, in accord with the determination of high volatile bituminous coal in volatile matter. Also, maceral analysis exhibits the minimum in exinite (<1.44%) and vitrinite is the dominant maceral varying from 76.88% to 78.77%, followed by inertinite (<16.55%), which is composed of a

Table 1: Proximate analysis and adsorption constant of coal samples.

Sample	Proximate analysis (wt.%)				Adsorption constant	
	Moisture	Ash	Volatile matter	Fixed carbon	V_L (m^3/t)	P_L (MPa)
XT-1	1.219	18.05	22.145	58.586	24.4684	1.6005
XT-2	1.105	15.52	20.6	62.775	24.1749	1.7733
XT-3	1.165	16.115	21.725	60.995	23.9867	1.6977
XT-4	1.043	15.865	23.17	59.922	23.8853	1.7021

macrinite and fusinite splitter. In addition, major inorganic components are made up of lump clay and finely granular sulfide. For pore structure analysis, the pore classification method proposed by B.B. Hodot is adopted to MIP data [41], which is presented in Figure 6(b). It can be concluded that the pore volume in the minipores and micropores account for more than 75%, and micropores are as well-developed as the primary pore ranged from 54.67% to 56.09%. To be specific, the comparison of pore volume shows a small difference between Redbed and normal zones. Overall, combined with the results in Table 1, it can be speculated that no obvious changes are observed in petrographic and pore structures of coal seam samples under the influence of Redbed.

4.2. Physical Properties of Caprocks

4.2.1. Pore Structure Analysis. Generally, pore structure is a fundamental factor for the research of gas diffusion and permeation on sealing capability. Scholars have proven that the diffusion coefficient of natural gas increased with porosity, irrelevant to rock property [42]. Also, the difference in permeability primarily depends on pore development for porous media [43]. Thereby, pore size distribution measurement can provide an important basis for evaluating the sealing capability of rocks [44]. Based on laboratory test, the relationship between incremental pore volume and pore diameter of rock samples from the surface drilling hole (74-11) is described in Figure 7.

As shown in Figure 7(a), there is an obvious change in pore size distributions of siltstone, sandstone, and mudstone. For sandstone, the curve shows multiple peaks in each phase, and mesopores and macropores are dominant in 10~5000 nm, which may illustrate that pore size distributions are discontinuous. Meanwhile, seepage-flow pores (>100 nm, mesopores and macropores) and adsorption pores (<100 nm, minipores and micropores) are well-developed, which deduces that gas migration in sandstone, i.e., permeation and diffusion behavior, is more prominent. For siltstone and mudstone, the pore size distributions show similar trends in adsorption pores (<100 nm, minipores and micropores). These results indicate that adsorption and diffusion behaviors are more dominant than that of permeation. Meanwhile, the pore size distribution of Redbed is exhibited in Figure 7(b). It can be speculated that minipores are abundant in the structure of Redbed, which is conductive to the diffusion process. Compared with Figures 7(a) and 7(b), it may be summarized that Redbed has the most influence on the promotion of gas diffusion and penetration, which is higher than sandstone; however, siltstone and mudstone with a less developed pore structure may not facilitate the gas migration.

4.2.2. Diffusion Analysis. The evaluation of the coal-bearing rocks (sandstone, mudstone, and siltstone), Paleogene rocks (Redbed), and Neogene and Quaternary rocks (loose bed) on gas diffusion and permeability can be considered as a guideline for gas accumulation and migration in coal seam, as well as the sealing capability of its overlying caprocks.

The diffusion coefficient is calculated through the counter diffusion method, which is derived from the diffusion concentration difference between both ends of the sample container. Following the gas diffusion in coal follows Fick's law; the diffusion coefficient can be fundamentally calculated as follows [39].

$$D = \frac{\ln\left(\Delta C_0/\Delta C_i\right)}{Et}, \tag{1}$$

$$E = \frac{A\left(1/V_1 + 1/V_2\right)}{l}, \tag{2}$$

where D is the diffusion coefficient, m^2/s; C is the gas concentration, mol/m^3; t is the diffusion time, s; ΔC_0 is the initial concentration difference, cm^3/cm^3, ΔC_i is the concentration difference at time i; A is the sectional area of the coal sample perpendicular to the diffusion direction, cm^2; l is the length of the sample, m; and V_1 and V_2 are the volumes of the diffusion cells, m.

According to Eq. (1) and Eq. (2), the relationship of the diffusion coefficient of sandstone, mudstone, siltstone, Redbed, and loose bed with confining pressure is presented in Figure 8. Overall, the diffusion coefficient could be generally ordered as sandstone > Redbed > loose bed > siltstone > mudstone. Under the same confining pressure, the diffusion coefficient of Redbed is close to that of sandstone and loose bed; however, it is approximately 15~20 times higher than the diffusion coefficient of siltstone and mudstone. Moreover, when the confining pressure is low, the difference in the diffusion coefficient between rock samples is more notable, whereas it gradually decreases with an increase in confining pressure. Therefore, it may be inferred that the rock samples of sandstone, Redbed, and loose bed have a positive effect on the gas diffusion, but siltstone and mudstone may hinder the gas migration in smaller pores. These findings were similar with the trend in the result of pore structure analysis except for the inconsistency in the sandstone, which may be due to the differences from the sample preparation.

4.2.3. Permeation Analysis. For the permeability test, Brace et al. [45] have firstly reported the transient pressure method that may determine the seepage properties of the sample. When comparing steady-state measurements, the transient pressure method is extensively accepted because of its shorter test durations and high precision [46, 47]. The decay curves of the differential pressure with the

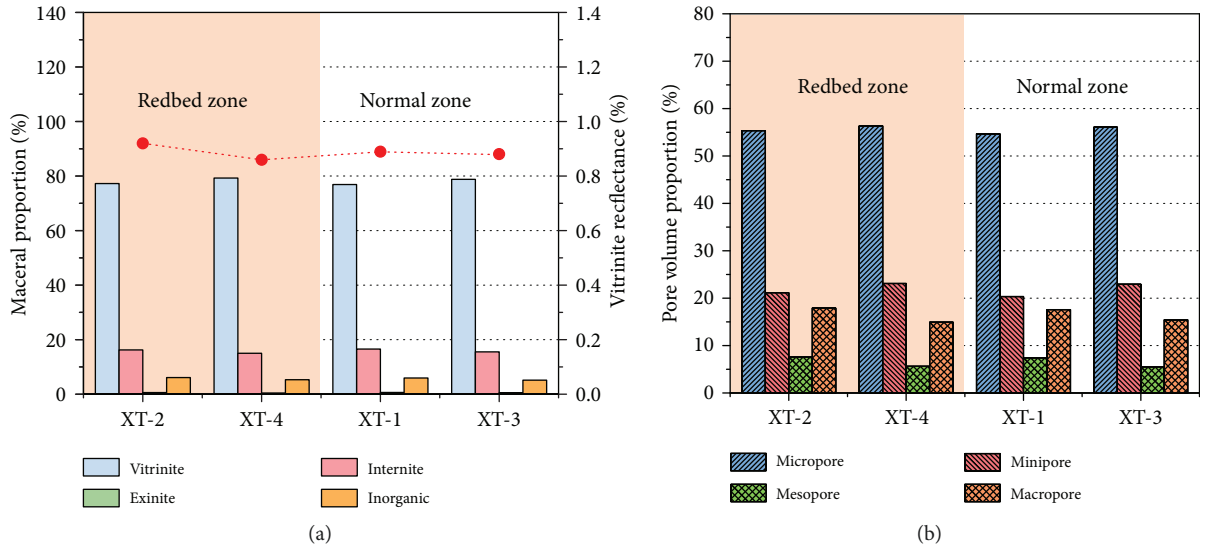

Figure 6: Petrographic (a) and pore structure (b) analyses of coal seam samples in the Xutuan coal mine.

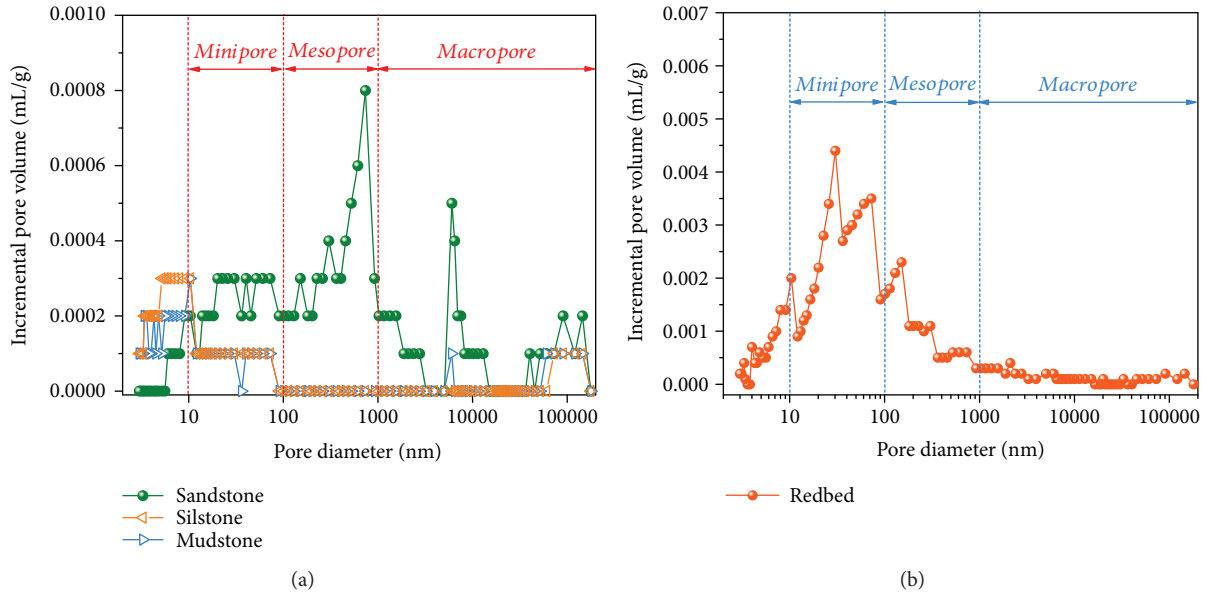

Figure 7: Pore size distributions of cap rock samples from the MIP method. (a) Sandstone, siltstone, and mudstone; (b) Redbed. Note: each rock sample is obtained from the coal-bearing strata and Redbed in the surface drilling hole of 74-11.

governing equations are adopted for the solution according to Eq. (3) and Eq. (4) [45, 47].

$$\frac{\Delta P(t)}{P_i} \propto e^{-\alpha t}, \tag{3}$$

$$\alpha = \frac{kA}{\mu C_g L}\left(\frac{1}{V_u} + \frac{1}{V_d}\right), \tag{4}$$

where $\Delta P(t)$ is the differential pressure up- and downstream at time t, in MPa; P_i is the initial differential pressure up- and downstream, in MPa; α is the exponential fitting factor of pressure with time; k is the permeability, in mD; A is the sectional area of rock samples, m^2; L is the length of rock samples, in m^2; μ is the dynamic viscosity, in MPa·s; C_g is the gas compressibility factor; and V_u and V_d are the volumes up- and downstream, respectively, in mL. Following Eq. (3) and Eq. (4), the changes of permeability of rock samples with confining pressure are exhibited in Figure 9.

As shown in Figure 9, it is obvious that permeability of the rock sample has the largest value in sandstone, followed by Redbed and loose bed, which are much larger than siltstone and mudstone. The order of magnitudes for sandstone, Redbed, and loose bed is 0.1 mD, which is almost a hundred times larger than that of siltstone and mudstone which is 0.001 mD. Similarly, the permeability of all rock samples shows a decreasing trend with confining pressure. Combined with the aforementioned results, it may be concluded that Redbed and loose bed are beneficial to gas diffusion and

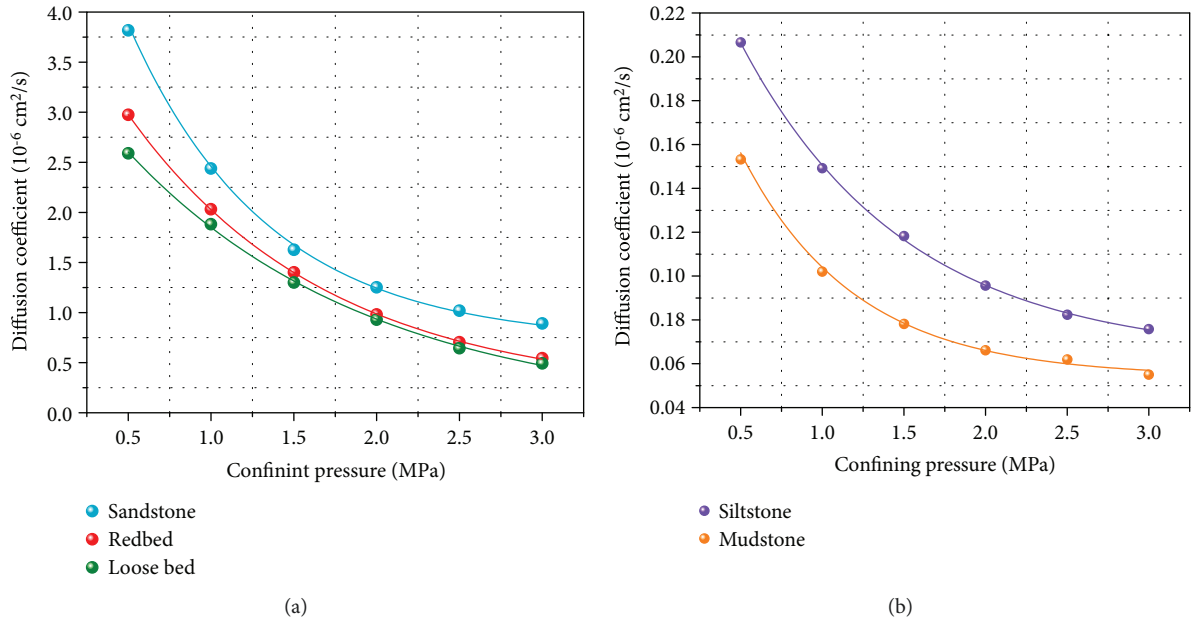

Figure 8: Diffusion coefficient of cap rock samples under different confining pressures. Note: loose bed refers to Quaternary and Neogene rocks; Redbed refers to Paleogene rock. The data points were derived from the average values of six surface drilling holes (75-7, 74-7, 74-11, 67-11, 73-14, and 75-8) that were calculated by the diffusion coefficients of the coal-bearing rocks (sandstone, mudstone, and siltstone), Paleogene rocks (Redbed), and Neogene and Quaternary rocks (Loose bed).

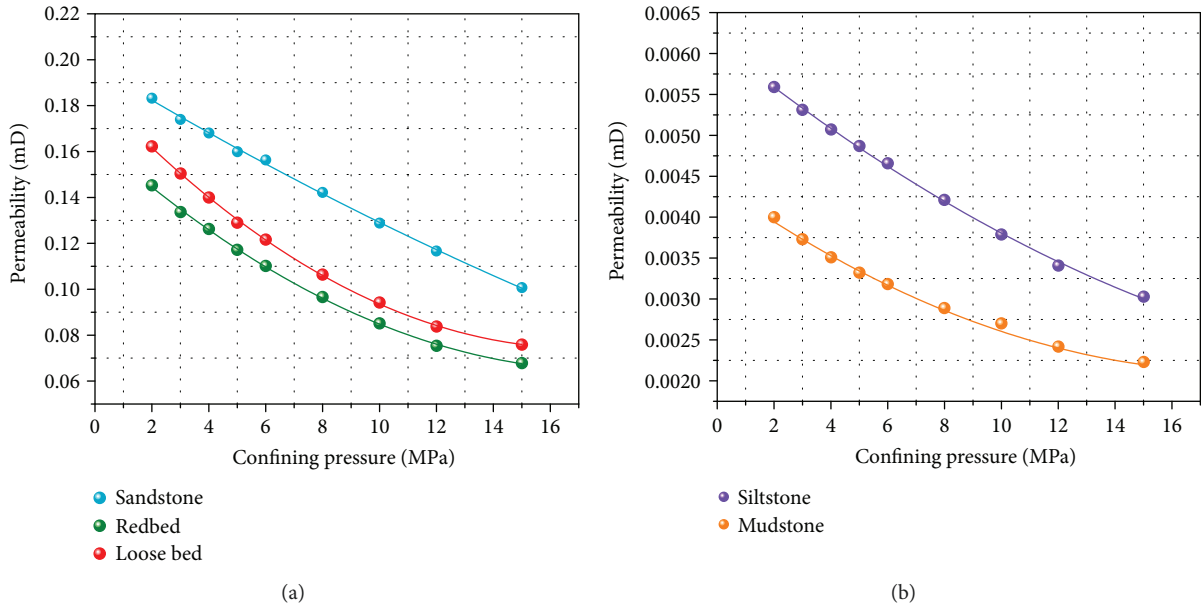

Figure 9: Permeability of cap rock samples under different confining pressures. Note: loose bed refers to Quaternary and Neogene rocks; Redbed refers to Paleogene rock. Note: the data points were derived from the average values of four surface drilling holes (75-7, 74-7, 74-11, 67-11, 73-14, and 75-8) that were calculated by the permeability of the coal-bearing rocks (sandstone, mudstone, and siltstone), Paleogene rocks (Redbed), and Neogene and Quaternary rocks (Loose bed).

seepage while mudstone and siltstone are not favorable for gas transport in the coal-bearing rocks.

5. Discussion

5.1. Impact of Loose Bed and Redbed on CBM Accumulation. The basic properties, petrography, and pore structure of the coal samples in the Xutuan coal mine, as discussed above, are not fundamentally altered in the presence of Redbed. From a view of geology, these findings may be related to the stratigraphic evolution of this area. Figure 10 presents the stratigraphic evolution of the coal-bearing strata in the Xutuan coal mine. The sedimentary process of the strata (Neogene and Quaternary, Paleogene, and coal-bearing

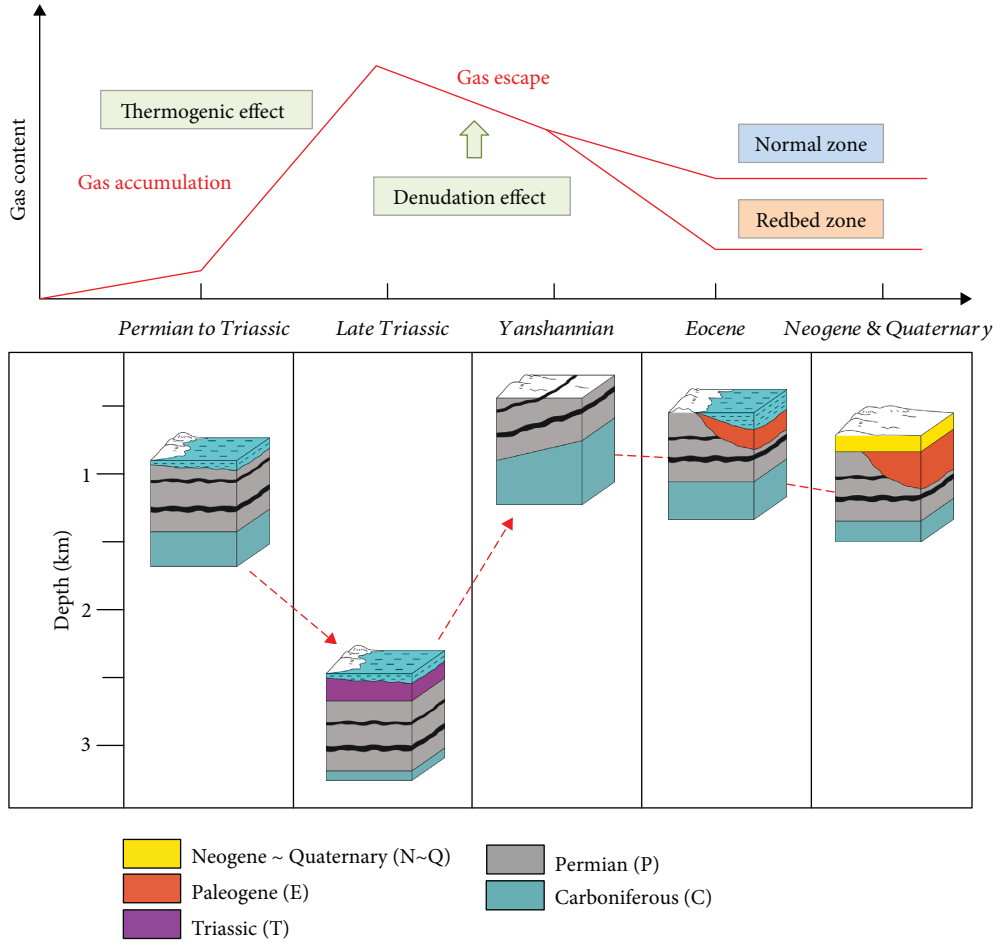

Figure 10: Schematic diagram exhibiting the stratigraphic evolution of the coal-bearing strata and the CBM accumulation process in the Xutuan coal mine. This is modified from Jin et al. [30].

formations) in the study area has roughly experienced five critical geological periods: Permian to Triassic, Late Triassic, Yanshannian, Eocene, and Neogene & Quaternary periods. The coal-bearing strata have undergone deposition, depression, uplifting, and erosion due to the impact of ground movements. Accordingly, the mechanism process of CBM accumulation from Permian to Yanshannian strongly depends on the gas generation and gas escape, which were caused by the thermogenic effect and the denudation effect, respectively. Notably, the thickness of the Permian strata in the Redbed zone was seriously denuded by erosion effects during the Mesozoic, leading to the emission of a mass of coalbed gas. On the contrary, the coalbed gas in the normal zone was preferably preserved without erosion effects. Thus, the geological effects during the stratigraphic evolution caused the difference of gas accumulation in the Redbed zone and normal zone.

Besides, no evidence has proven the existence of large-scale open faults in the underlying coal seam whether it is under normal or Redbed zone, which may be thought as the same geological unit with a similar coal-forming period and gas-generating stage. However, the gas emission quantity decreases with an increase in the deposit thickness of Redbed, which has been reported in a previous study [30]. Redbed can serve as a permeable medium with high-porosity and high-permeability properties that may hinder coalbed gas accumulation and is favorable for gas diffusion and seepage [30]. Simultaneously, as mentioned above, the analysis of diffusion and seepage characteristics on the caprocks has demonstrated that the diffusion coefficient and permeability of Redbed under the same confining pressure are not only close to loose bed, but are much greater than those in siltstone and mudstone. Similar to Redbed, loose bed may be deduced as a well-developed porous layer with a poor sealability. Provided that there is little difference in the total thickness of caprocks, the coexistence of Neogene and Quaternary rocks (Loose bed) and Paleogene rocks (Redbed) may ultimately contribute to CBM migration in this studying area. More similarities in physical properties of Redbed and loose bed, as well as their influences on gas accumulation, may basically provide evidence for treating both things as a whole, which are valuable for exploring the sealability evaluation of caprocks for coal seam.

5.2. Sealing Mechanism of Caprocks on CBM Migration. It has been widely accepted that the majority of coalbed gas, generated from coalification of source rocks (coal) during the long-term geological history, is inclined to accumulate due to the

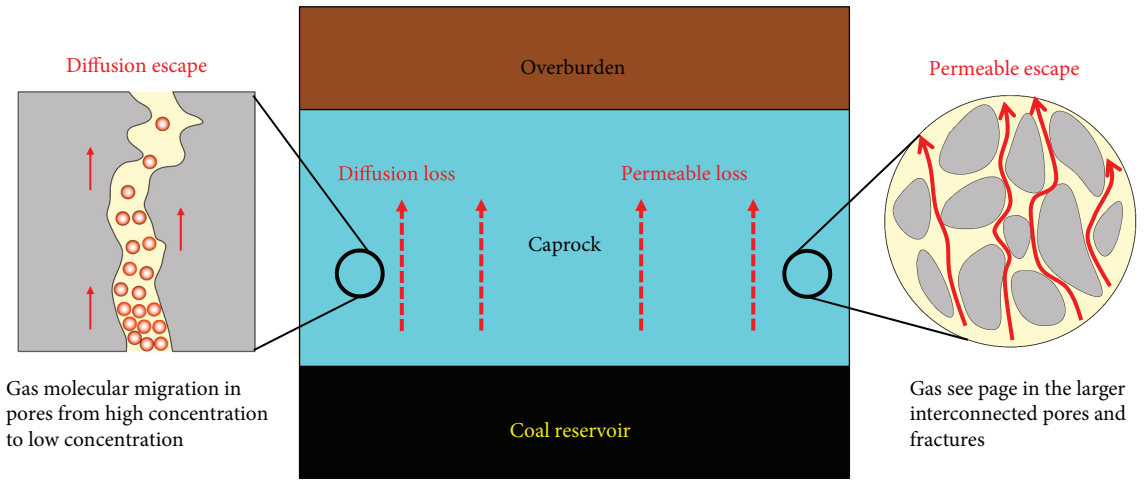

Figure 11: Conceptional diagram showing the sealing mechanism of caprocks and its effect on CBM migration.

good seal condition of coal-bearing strata overlying and underlying coal seam. However, it has been proven that gas storage capacity is below gas-generated quantity in coal seam only if coalbed gas escapes, i.e., transports from coal seam towards overlying strata, which is a dominating factor on a geological timescale [29]. Song and Zhang [14] proposed possible leakage pathways after long-term CO_2 geological sequestration, which are categorized as the leakage in faults or fractures, concentration gradient controlling leakage (diffusion loss), and leakage controlled by capillary pressure (permeable loss). For coalbed gas, the transport mechanism in coal seam can be principally defined as diffusion escape and permeable escape, which are presented in Figure 11. Diffusion escape occurs mainly in the pore structure of caprock matrices from high concentration to low concentration. In this case, coalbed gas could diffuse through caprock in the form of molecular migration, which is permanent and slow with concentration difference [48]. The capacity of the diffusion escape process relies on the diffusion coefficient of caprocks. Meanwhile, larger interconnected pores and fractures in caprocks may act as the major channels for gas seepage, the capacity of which could be enhanced by high pressure [49]. However, capillary sealing may prevent gas flow upward when the gas pressure is below the breakthrough pressure [50, 51]. Accordingly, capillary pressure is confirmed to be dominated in permeable escape and is controlled by permeability of caprocks. Furthermore, the sealability of caprock is closely related to rock types, thickness, and fracture development; specifically, thickness can be thought as one of the key control factors [14]. In other words, the above statements can be summarized that the sealability of caprocks is determined by three factors: thickness, permeation, and diffusion features of overlying strata.

From the macroscopic perspective, it is accepted that abundant coalbed gas may accumulate in coal seam when the overlying direct roof and underlying direct floor have good sealing capacity; however, if one of the adjacent strata has poor sealing capacity, low gas content may occur in coal seam [52]. The overlying roof and underlying floor are both significant for CBM accumulation; however, the roof has a more predominant effect on gas migration by reason of the spontaneous upward movement of coalbed gas [53]. Considering the actual geological condition of the study area, semi-quantitative evaluation of sealing ability in the caprocks could be further carried out from model simplification and theoretical calculation through the aforementioned findings in relation to the diffusion and permeability of rocks, coupled with sealing mechanisms on caprocks.

5.3. Conceptional Analysis on the Sealing Ability of Caprock

5.3.1. Simplification of Caprock Thickness. In the study area, the coal seam is overlain by interbedded coal-bearing strata (primarily composed sandstone, mudstone, and siltstone), which refer to extensive thickness and complexity in the lithological sequences and are not beneficial to stratigraphic scientific analysis. The conceptional lithological sequences of caprocks in this area may be supposedly displayed as in Figure 12(a). In this case, to better evaluate the sealing ability of caprocks in different areas, the mudstone, sandstone, and siltstone in the surface drilling holes, interbedded in the coal-bearing strata, may be assumed to be the simplified caprocks with homogeneous features, which contains three basic units: mudstone strata, sandstone strata, and siltstone strata. As illustrated in Figure 12(b), the coal-bearing strata (total thickness of all rocks is l) may be simplified into i mudstone strata (each thickness is l_i and total thickness is l_{mu}), j sandstone strata (each thickness is l_j and total thickness is l_{sa}), and k siltstone strata (each thickness is l_k and total thickness is l_{si}). In addition, the thickness of the Redbed and loose bed are l_{re} and l_{lo}, respectively. Derived from the surface drilling holes in Figure 2, the thickness of each rock sample could be summarized as in Table 2. Due to the heterogeneity in rock property, the overlying strata can be divided into several vertical layers; thereby, methods will be simplified as the analysis of multilayer composite porous media flow.

5.3.2. Comparison on the Sealability of the Simplified Caprocks. It has been discussed above that regardless of the

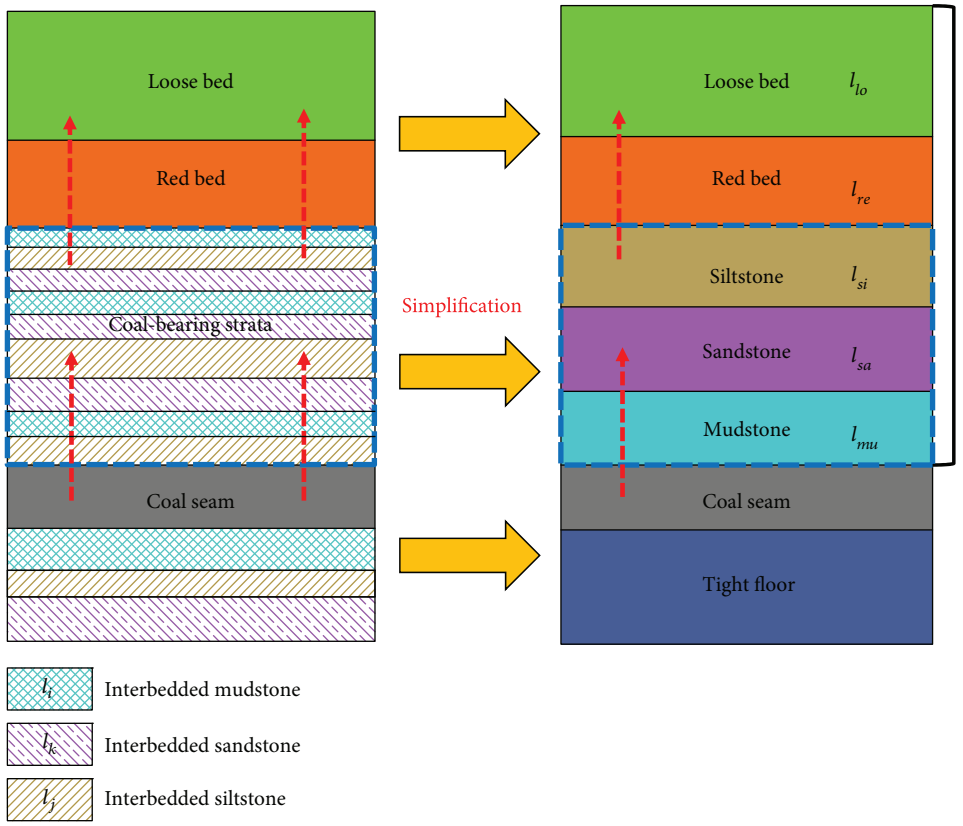

Figure 12: Conceptional lithological sequences of caprocks and the simplification model.

Table 2: The total thickness of each cap rock from surface drilling holes.

Surface drilling	l_{lo} (m)	l_{re} (m)	l_{sa} (m)	l_{si} (m)	l_{mu} (m)
75-7	351.6	80.1	31.6	8.6	33.3
74-7	434.2	0	41.1	62.2	41.1
74-11	354.5	32.5	46.2	27.1	114.7
67-11	350.1	55.2	24.9	46.4	120.7
73-14	348.2	0	18.4	66.7	138.6
75-8	386.7	108	35.2	26.3	55.8

thickness, the sealing capability of caprocks is mainly affected by two factors: diffusion and seepage properties. For diffusion, migration behavior in rocks obeys Fick's law when a concentration difference exists. Thus, coalbed gas may possibly transport upwards the caprocks through mudstone (l_{mu}), sandstone (l_{sa}), and siltstone (l_{si}), and then potentially pass across Redbed (l_{re}) and loose bed (l_{lo}), as shown in Figure 12. Associated with the diffusion theory in porous media, the average diffusion factor (D) of the overlying strata can be expressed as Eq. (5):

$$\frac{l}{D} = \sum_{i=1}^{u} \frac{l_i}{D_{sa}} + \sum_{j=1}^{v} \frac{l_j}{D_{si}} + \sum_{k=1}^{w} \frac{l_k}{D_{mu}}, \quad (5)$$

where D_{sa}, D_{si}, and D_{mu} are the diffusion coefficient of sandstone, siltstone, and mudstone, respectively.

To simplify the calculation, the thickness was assumed as a small value, and the diffusion coefficient of each rock was defined as a constant. According to the series connection theory, the simplified average diffusion factor could be presented as Eq. (6):

$$\frac{l}{D} = \frac{l_{sa}}{D_{sa}} + \frac{l_{si}}{D_{si}} + \frac{l_{mu}}{D_{mu}}. \quad (6)$$

For seepage in rocks, the transport pathway of coalbed gas is similar to that of diffusion. The seepage law of caprocks may be explained by the multilayer composite linear seepage equation, which is deduced as follows. Flow through the cleat system of rocks is pressure-driven and can be described using Darcy's law, which is expressed as Eq. (7):

$$v = -\frac{k}{\mu} \cdot (\nabla p + \rho g \nabla z), \quad (7)$$

where k is the permeability, in mD; v is the gas velocity, in m/s; μ is the methane viscosity, in Pa·s; p is the gas pressure, in MPa; g is the gravitational acceleration, in m·s^{-2}; ∇p means the derivative of p with respect to the migration path, and ∇z is equal to $\{0 \quad 0 \quad 1\}^T$ which can be immediately removed after subsequent calculations. In many situations, the gravitational term is thought to be relatively small, and the contribution of gas density on the Darcy velocity is relatively small compared to that of the gas pressure. Thus, in

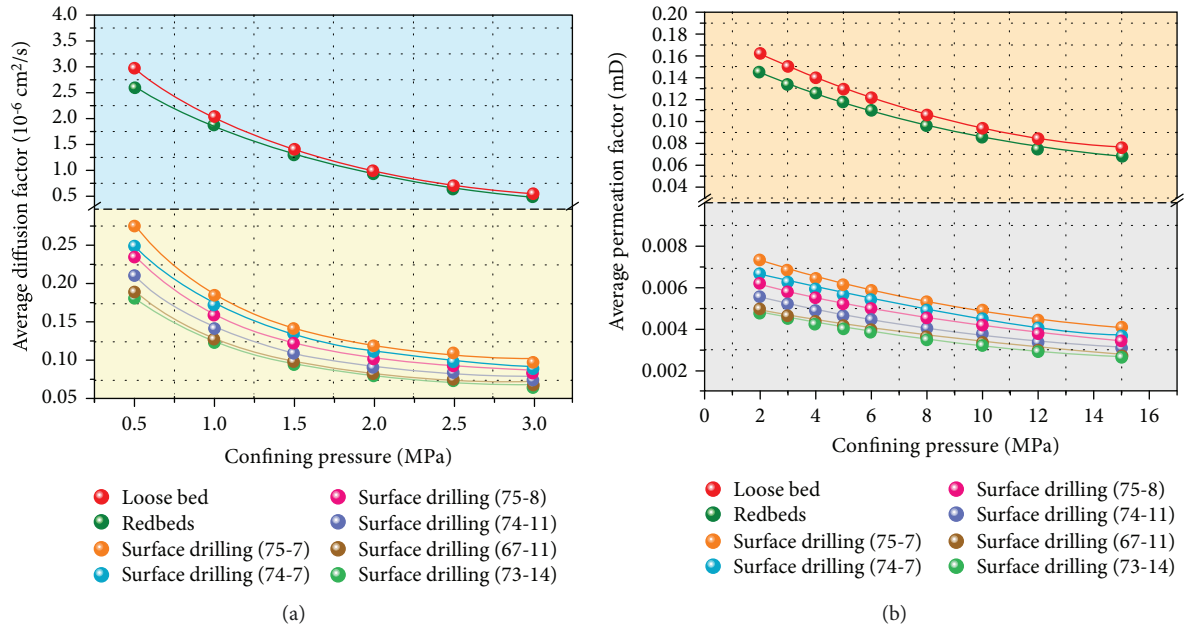

Figure 13: Changes of average diffusion and permeation factors of loose bed, Redbed, and surface drilling holes (coal-bearing strata). Note: loose bed refers to Quaternary and Neogene rocks; Redbed refers to Paleogene rock.

this case, the gravitational term may be ignored to facilitate calculation [54, 55].

Combined with the equation of motion, the flow formula is listed as Eq. (8):

$$qB = Av = wh\frac{k}{\mu}\frac{\Delta p}{l}, \tag{8}$$

where q is the quantity of gas flow; B is the volume coefficients of gas flow; A is the cross-sectional area of the whole strata; w and h are the length and width of the whole strata; and Δp is the pressure difference at both ends of the whole strata.

In this case, it can be considered that for each stratum, the overlays of the flow formula based on the equation of motion are equal to the integral flow formula, as shown in Eq. (9).

$$qB = wh\frac{\Delta p}{\mu\sum_{i=1}^{n}(l_i/k_i)} = whk\frac{\Delta p}{\mu l}, \tag{9}$$

where l_i is the thickness of each stratum; k_i is the permeability of each rock; and k is the average permeation factor of the whole strata.

Therefore, the average permeation factor of total layers (k) is obtained from Eq. (9):

$$k = \frac{l}{\sum_{i=1}^{n}(l_i/k_i)}. \tag{10}$$

In this regard, coupled with the experimental results on the diffusion coefficient and permeability of all rock samples in Section 4.2, Eq. (6) and Eq. (10) are used to obtain the changes of the average diffusion factor and average permeation factor of the coal-bearing strata with pressure, respectively. As shown in Figure 13, it is apparent that the diffusion coefficient and permeability of Redbed and loose bed are much greater than that of coal-bearing rocks, which exhibits a slight difference on each surface drilling hole, with an order of 75-7 > 74-7 > 74-11 > 75-8 > 67-11 > 73-14. Thus, the arithmetic mean value of the average diffusion factor and average permeation factor for all surface drilling holes in the field could be adopted as the guiding values on evaluating the diffusion coefficient and permeability for the whole caprocks in the study area, respectively. Also, it can be verified from Figure 13 that the average diffusion factor and average permeation factor decrease with an increase in pressure, indicating that the confining pressure has a positive effect on the sealing capacity of caprock. By comparing the diffusion coefficient and permeability of coal-bearing rocks with Redbed and loose bed, the sealing ability of overlying strata on coalbed gas may be evaluated directly.

However, due to the complexity of actual strata, the real effective confining pressure is inaccessible to acquire. Also, because of the various burial depth for coal-bearing strata, changes in the diffusion coefficient and permeability of caprock may be more complicated. Despite these, it is more convenient to contrast relatively with the strata types in terms of average diffusion and permeation factors of the caprocks deduced from the above discussion. That is, Redbed and loose bed have a poor sealability on coalbed gas while coal-bearing strata play an important role in CBM accumulation. In summary, it can be inferred from the discussion that Redbed and loose bed have no direct influence on CBM accumulation unless the increasing burial depth enhanced the sealability of caprock through strong geostress. Therefore, the key controlling factor for CBM accumulation may be attributed to the coal-bearing strata. Abilities of CBM migration towards overlying strata in relation to the diffusion and seepage properties

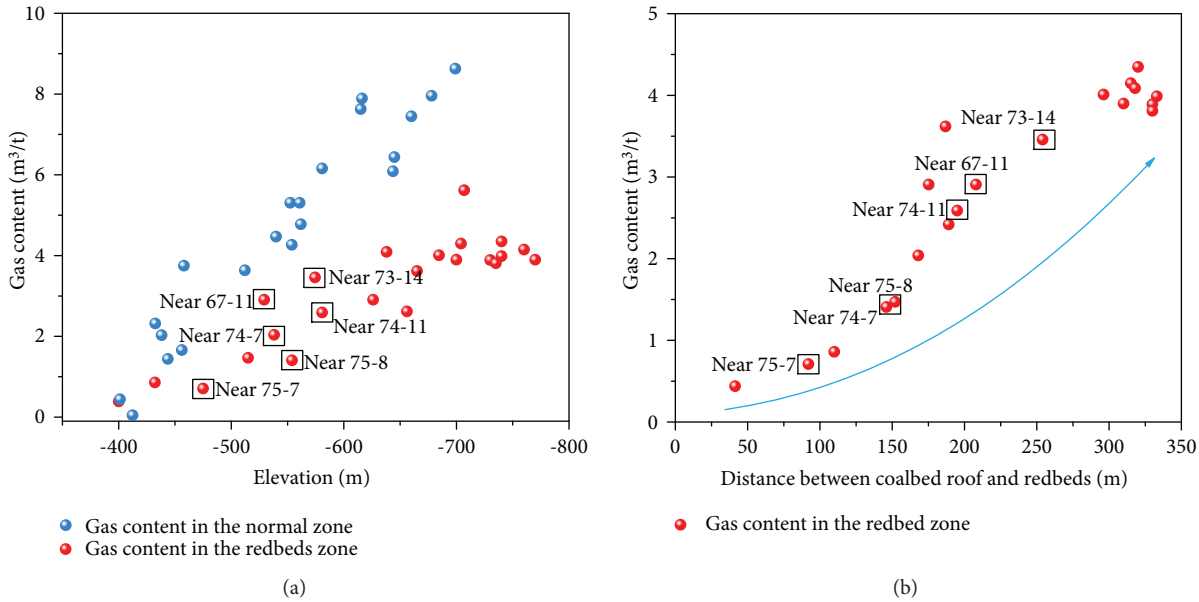

Figure 14: Verification of the in-place gas content in the field: (a) relationship between gas content and elevation, and (b) relationship between gas content and caprock isopach.

are governed by the types and thickness of cap rocks, which are favorable for CBM generation and accumulation.

5.3.3. Field Test and Verification. To verify the gas-escaping effect of Redbed and loose bed, and the overlying caprock on coalbed gas accumulation, as well as the reliability of sealability evaluation on the average diffusion factor and average permeation factor, a direct method for the in-place gas content is used through the coal samples underground drilling holes during coal mine production [56]. Simultaneously, the corresponding burial depth with pressure and temperature was recorded. Also, the isopach between coal seam roof and Redbed was analyzed and is displayed in Figure 2. The relationship of in-place gas content, elevation, and caprock isopach is presented in Figures 14(a) and 14(b).

As shown in Figure 14(a), the in-place gas content in the field increases with burial depth. The in-place gas content of the Redbed zone is somewhat below the normal zone in the presence of Redbed, and the gap may widen between Redbed and normal zones with the burial depth of the coal seam. Nevertheless, it is clearer to figure out that the key factor on coalbed gas accumulation is not only the burial depth but also the thickness of the overlying caprock, for the explanation that the in-place gas content in the Redbed zone increases effectively with the isopach between coal seam roof and Redbed, as described in Figure 14(b). More specifically, six surface drilling holes (75-7, 74-7, 74-11, 67-11, 73-14, and 75-8) are marked in Figure 14(a) where those are near the actual points of the in-place gas content. Results show that although overall data exhibits a positive correlation, the in-place gas content data ranging from small to large are not completely consistent with burial depth from shallow to deep. However, the in-place gas contents are more accurately ordered by the thickness of the overlying coal-bearing strata, i.e., 75-7 < 74-7 < 75-8 < 74-11 < 67-11 < 73-14 (from thin to thick). This may suggest a direct reflection on the in-place gas content and be coincided with the practical situation in Section 5.3.2, which are an important verification for sealability of overlying caprocks with evaluation.

6. Conclusion

Xutuan coal mine, Huaibei Coalfield, China, has been confirmed to have extensive distributions of Redbed and loose bed overlying the coal seam, which serve as a permeable medium and are suitable for CBM migration. However, the coal-bearing strata, mostly consisting of mudstone, siltstone, and sandstone with lower permeability, may supply a good sealing condition for CBM accumulation in coal seam. In this case, the physical and lithology properties of coal and cap rocks were characterized by laboratory tests, theoretical analysis, and on-site exploration. Investigation on the key factors, i.e., thickness, diffusion coefficient, and permeability of overlying caprock, is valuable for a theoretical estimate of sealability. Here, major conclusions are drawn as follows:

For basic properties of coal, the Redbed has no impact on the proximate analysis, adsorption constant, maceral content, and pore development. The pore structure analysis of caprocks indicates that Redbed has a more developed pore connectivity than sandstone while siltstone and mudstone exhibits poor developmental features. The experimental observation of overlying caprocks based on the counterdiffusion method proves that the diffusion coefficient gradually decreases as the confining pressure increases with an order of sandstone > Redbed > loose bed > siltstone > mudstone. It is notable that sandstone, Redbed, and loose bed change markedly when compared to siltstone and mudstone. Similar trends were found in the permeability of overlying caprocks according to the transient pressure method. Furthermore, the sealing mechanism of caprocks provides a schematic knowledge of the CBM accumulation and migration process, demonstrating that the key factors affecting the sealability are

the thickness, diffusion, and seepage properties. Thus, with a simplification on the thickness of caprocks, the average diffusion factor and average permeation factor were put forward to theoretically evaluate the sealing capacity of caprocks. Through the conceptional analyses on the overlying caprocks of surface drilling holes, the diffusion and seepage capacities of coal-bearing strata are far less than those of Redbed and loose bed. The master factor on CBM accumulation may be attributed to the coal-bearing strata. Moreover, the newly proposed evaluation method on sealability coupled with the gas accumulation and migration mechanism was accurately verified by the field test of gas content in the actual coal seam.

Data Availability

The data in figures and tables used to support the findings of this study have not been made available due to the commercial agreement with Xutuan coal mine. Requests for data, 24 months after publication of this article, will be considered by the corresponding authors.

Conflicts of Interest

The authors declare no competing financial interest.

Acknowledgments

This research was supported by the National Natural Science Foundation of China (No. 51674252 and No. 51574229), the Fundamental Research Funds for the Central Universities (grant 2015XKMS006), the Qing Lan Project, Six Talent Peaks Project in Jiangsu Province (GDZB-027), the sponsorship of Jiangsu Overseas Research & Training Program for University Prominent Young & Middle-Aged Teachers and Presidents, and a project funded by the Priority Academic Program Development of Jiangsu Higher Education Institutions (PAPD).

References

[1] S. Kirschke, P. Bousquet, P. Ciais et al., "Three decades of global methane sources and sinks," *Nature Geoscience*, vol. 6, no. 10, pp. 813–823, 2013.

[2] I. Palmer, "Coalbed methane completions: a world view," *International Journal of Coal Geology*, vol. 82, no. 3-4, pp. 184–195, 2010.

[3] S. Dai and R. B. Finkelman, "Coal geology in China: an overview," *International Geology Review.*, vol. 60, no. 5-6, pp. 531–534, 2018.

[4] Y. Qin, T. A. Moore, J. Shen, Z. Yang, Y. Shen, and G. Wang, "Resources and geology of coalbed methane in China: a review," *International Geology Review*, vol. 60, no. 5-6, pp. 777–812, 2018.

[5] H. Li, H. C. Lau, and S. Huang, "China's coalbed methane development: a review of the challenges and opportunities in subsurface and surface engineering," *Journal of Petroleum Science and Engineering*, vol. 166, no. 1, pp. 621–635, 2018.

[6] B. B. Beamish and P. J. Crosdale, "Instantaneous outbursts in underground coal mines: an overview and association with coal type," *International Journal of Coal Geology*, vol. 35, no. 1-4, pp. 27–55, 1998.

[7] J. Liu, R. Zhang, D. Song, and Z. Wang, "Experimental investigation on occurrence of gassy coal extrusion in coalmine," *Safety science*, vol. 113, pp. 362–371, 2019.

[8] X. Chai, D. J. Tonjes, and D. Mahajan, "Methane emissions as energy reservoir: context, scope, causes and mitigation strategies," *Progress in Energy and Combustion Science*, vol. 56, pp. 33–70, 2016.

[9] H. Jianchao, W. Zhiwei, and L. Pingkuo, "Current states of coalbed methane and its sustainability perspectives in China," *International Journal of Energy Research*, vol. 42, no. 11, pp. 3454–3476, 2018.

[10] C. Ö. Karacan, F. A. Ruiz, M. Cotè, and S. Phipps, "Coal mine methane: a review of capture and utilization practices with benefits to mining safety and to greenhouse gas reduction," *International Journal of Coal Geology*, vol. 86, no. 2-3, pp. 121–156, 2011.

[11] J. C. Pashin, M. R. McIntyre-Redden, S. D. Mann, D. C. Kopaska-Merkel, M. Varonka, and W. Orem, "Relationships between water and gas chemistry in mature coalbed methane reservoirs of the Black Warrior Basin," *International Journal of Coal Geology*, vol. 126, pp. 92–105, 2014.

[12] J. Zhang, D. Liu, Y. Cai, Z. Pan, Y. Yao, and Y. Wang, "Geological and hydrological controls on the accumulation of coalbed methane within the no. 3 coal seam of the southern Qinshui Basin," *International Journal of Coal Geology*, vol. 182, pp. 94–111, 2017.

[13] J. Rutqvist and C.-F. Tsang, "A study of caprock hydromechanical changes associated with CO_2-injection into a brine formation," *Environmental Geology*, vol. 42, no. 2-3, pp. 296–305, 2002.

[14] J. Song and D. Zhang, "Comprehensive review of caprock-sealing mechanisms for geologic carbon sequestration," *Environmental science & technology*, vol. 47, no. 1, pp. 9–22, 2012.

[15] Y. Li, D. Tang, P. Wu et al., "Continuous unconventional natural gas accumulations of Carboniferous-Permian coal-bearing strata in the Linxing area, northeastern Ordos basin, China," *Journal of Natural Gas Science and Engineering*, vol. 36, pp. 314–327, 2016.

[16] G. Liu, M. Sun, Z. Zhao, X. Wang, and S. Wu, "Characteristics and accumulation mechanism of tight sandstone gas reservoirs in the Upper Paleozoic, northern Ordos Basin, China," *Petroleum Science*, vol. 10, no. 4, pp. 442–449, 2013.

[17] X. Tang, J. Zhang, X. Wang et al., "Shale characteristics in the southeastern Ordos Basin, China: implications for hydrocarbon accumulation conditions and the potential of continental shales," *International Journal of Coal Geology*, vol. 128-129, pp. 32–46, 2014.

[18] R. Li, K. Jin, and D. J. Lehrmann, "Hydrocarbon potential of Pennsylvanian coal in Bohai Gulf Basin, Eastern China, as revealed by hydrous pyrolysis," *International Journal of Coal Geology*, vol. 73, no. 1, pp. 88–97, 2008.

[19] K. W. Shanley, R. M. Cluff, and J. W. Robinson, "Factors controlling prolific gas production from low-permeability sandstone reservoirs: implications for resource assessment, prospect development, and risk analysis," *AAPG bulletin*, vol. 88, no. 8, pp. 1083–1121, 2004.

[20] Y. Chen, D. Tang, H. Xu, Y. Li, and Y. Meng, "Structural controls on coalbed methane accumulation and high production models in the eastern margin of Ordos Basin, China," *Journal*

of Natural Gas Science and Engineering, vol. 23, pp. 524–537, 2015.

[21] H. Wang, Y. Yao, D. Liu, Z. Pan, Y. Yang, and Y. Cai, "Fault-sealing capability and its impact on coalbed methane distribution in the Zhengzhuang field, southern Qinshui Basin, North China," *Journal of Natural Gas Science and Engineering*, vol. 28, pp. 613–625, 2016.

[22] Z. Yang, Y. Qin, G. X. Wang, and H. An, "Investigation on coal seam gas formation of multi-coalbed reservoir in Bide-Santang Basin Southwest China," *Arabian Journal of Geosciences*, vol. 8, no. 8, pp. 5439–5448, 2015.

[23] Z. Chen, F. Zhou, and S. S. Rahman, "Effect of cap rock thickness and permeability on geological storage of CO2: laboratory test and numerical simulation," *Energy Exploration & Exploitation*, vol. 32, no. 6, pp. 943–964, 2014.

[24] A.-A. Grimstad, S. Georgescu, E. Lindeberg, and J.-F. Vuillaume, "Modelling and simulation of mechanisms for leakage of CO2 from geological storage," *Energy Procedia*, vol. 1, no. 1, pp. 2511–2518, 2009.

[25] W. Li, C. Y-p, L. Wang, Z. H-x, W. H-f, and W. L-g, "Evaluating the security of geological coalbed sequestration of supercritical CO_2 reservoirs: the Haishiwan coalfield, China as a natural analogue," *International Journal of Greenhouse Gas Control*, vol. 13, pp. 102–111, 2013.

[26] W. Li, P. L. Younger, Y. Cheng et al., "Addressing the CO 2 emissions of the world's largest coal producer and consumer: lessons from the Haishiwan Coalfield, China," *Energy*, vol. 80, pp. 400–413, 2015.

[27] M. N. Watson, N. Zwingmann, and N. M. Lemon, "The Ladbroke Grove–Katnook carbon dioxide natural laboratory: a recent CO 2 accumulation in a lithic sandstone reservoir," *Energy*, vol. 29, no. 9-10, pp. 1457–1466, 2004.

[28] H. Feng, S. Yan, Z. Mengjun, L. Shaobo, Q. Shengfei, and F. Guoyou, "Cap rock influence on coalbed gas enrichment in Qinshui Basin," *Natural Gas Industry*, vol. 25, no. 12, p. 34, 2005.

[29] S. Shuxun, F. Bingheng, Q. Yong, T. Shuheng, Y. Jianping, and J. Shetun, "Conditions of seal- ing and accumulation in coalbed gas," *Oil & Gas Geology*, vol. 20, no. 2, pp. 104–107, 1999.

[30] K. Jin, Y. Cheng, L. Wang et al., "The effect of sedimentary redbeds on coalbed methane occurrence in the Xutuan and Zhaoji Coal Mines, Huaibei Coalfield, China," *International Journal of Coal Geology*, vol. 137, pp. 111–123, 2015.

[31] B. Besly, *Palaeogeographic Implications of Late Westphalian to Early Permian Red-Beds, Central England. Sedimentation in a Synorogenic Basin Complex: the Upper Carboniferous of Northwest Europe Blackie*, Blackie, Glasgow, 1988.

[32] J. Rong, Y. Wang, and X. Zhang, "Tracking shallow marine red beds through geological time as exemplified by the lower Telychian (Silurian) in the Upper Yangtze Region, South China," *Science China Earth Sciences*, vol. 55, no. 5, pp. 699–713, 2012.

[33] L. Liu, X. Shang, Y. Wang et al., "Controlling factors on oil and gas accumulation and accumulation modes of the Paleogene "Red Bed" in the South Slope of the Dongying Depression, China," *Energy Exploration & Exploitation*, vol. 30, no. 6, pp. 941–956, 2012.

[34] L. Wang, C. Y-p, F.-h. An, Z. H-x, K. S-l, and W. Wang, "Characteristics of gas disaster in the Huaibei coalfield and its control and development technologies," *Natural hazards*, vol. 71, no. 1, pp. 85–107, 2014.

[35] L. Wang, C. Y-p, C. Xu, F.-h. An, K. Jin, and Z. X-l, "The controlling effect of thick-hard igneous rock on pressure relief gas drainage and dynamic disasters in outburst coal seams," *Natural Hazards*, vol. 66, no. 2, pp. 1221–1241, 2013.

[36] X. Tan, K. P. Kodama, H. Chen, D. Fang, D. Sun, and Y. Li, "Paleomagnetism and magnetic anisotropy of cretaceous red beds from the Tarim basin, Northwest China: evidence for a rock magnetic cause of anomalously shallow paleomagnetic inclinations from central Asia," *Journal of Geophysical Research: Solid Earth*, vol. 108, no. B2, 2003.

[37] S. Ting, G. J. Bowen, P. L. Koch et al., "Biostratigraphic, chemostratigraphic, and magnetostratigraphic study across the Paleocene-Eocene boundary in the Hengyang Basin, Hunan, China," in *Special Paper 369: Causes and Consequences of Globally Warm Climates in the Early Paleogene*, pp. 521–536, Geological Society of America, 2003.

[38] K. Zhang, Y. Cheng, W. Li, D. Wu, and Z. Liu, "Influence of supercritical CO_2 on pore structure and functional groups of coal: implications for CO_2 sequestration," *Journal of Natural Gas Science and Engineering*, vol. 40, pp. 288–298, 2017.

[39] J. Dong, Y. Cheng, Q. Liu, H. Zhang, K. Zhang, and B. Hu, "Apparent and true diffusion coefficients of methane in coal and their relationships with methane desorption capacity," *Energy & Fuels*, vol. 31, no. 3, pp. 2643–2651, 2017.

[40] H. Chen, Y. Cheng, T. Ren, H. Zhou, and Q. Liu, "Permeability distribution characteristics of protected coal seams during unloading of the coal body," *International Journal of Rock Mechanics and Mining Sciences*, vol. 71, pp. 105–116, 2014.

[41] Y. Cai, D. Liu, Z. Pan, Y. Yao, J. Li, and Y. Qiu, "Pore structure and its impact on CH 4 adsorption capacity and flow capability of bituminous and subbituminous coals from Northeast China," *Fuel*, vol. 103, pp. 258–268, 2013.

[42] H. Xu, D. Tang, J. Zhao, S. Li, and S. Tao, "A new laboratory method for accurate measurement of the methane diffusion coefficient and its influencing factors in the coal matrix," *Fuel*, vol. 158, pp. 239–247, 2015.

[43] C. M. White, D. H. Smith, K. L. Jones et al., "Sequestration of carbon dioxide in coal with enhanced coalbed methane recovery a review," *Energy & Fuels*, vol. 19, no. 3, pp. 659–724, 2005.

[44] J. E. Heath, T. A. Dewers, B. J. McPherson et al., "Pore networks in continental and marine mudstones: characteristics and controls on sealing behavior," *Geosphere*, vol. 7, no. 2, pp. 429–454, 2011.

[45] W. F. Brace, J. Walsh, and W. Frangos, "Permeability of granite under high pressure," *Journal of Geophysical research*, vol. 73, no. 6, pp. 2225–2236, 1968.

[46] Q. Liu, Y. Cheng, T. Ren, H. Jing, Q. Tu, and J. Dong, "Experimental observations of matrix swelling area propagation on permeability evolution using natural and reconstituted samples," *Journal of Natural Gas Science and Engineering*, vol. 34, pp. 680–688, 2016.

[47] Z. Pan, L. D. Connell, and M. Camilleri, "Laboratory characterisation of coal reservoir permeability for primary and enhanced coalbed methane recovery," *International Journal of Coal Geology*, vol. 82, no. 3-4, pp. 252–261, 2010.

[48] I. Gaus, "Role and impact of CO 2–rock interactions during CO 2 storage in sedimentary rocks," *International journal of greenhouse gas control*, vol. 4, no. 1, pp. 73–89, 2010.

[49] E. Kreft, C. Bernstone, R. Meyer et al., ""The Schweinrich structure", a potential site for industrial scale CO 2 storage and a test case for safety assessment in Germany," *International*

Journal of Greenhouse Gas Control, vol. 1, no. 1, pp. 69–74, 2007.

[50] A. Hildenbrand, S. Schlömer, and B. Krooss, "Gas breakthrough experiments on fine-grained sedimentary rocks," *Geofluids*, vol. 2, no. 1, 23 pages, 2002.

[51] A. Hildenbrand, S. Schlömer, B. Krooss, and R. Littke, "Gas breakthrough experiments on pelitic rocks: comparative study with N_2, CO_2 and CH_4," *Geofluids*, vol. 4, no. 1, 80 pages, 2004.

[52] Z. Zhang, Y. Qin, X. Fu, Z. Yang, and C. Guo, "Multi-layer superposed coalbed methane system in southern Qinshui Basin, Shanxi Province, China," *Journal of Earth Science*, vol. 26, no. 3, pp. 391–398, 2015.

[53] R. Shukla, P. Ranjith, A. Haque, and X. Choi, "A review of studies on CO 2 sequestration and caprock integrity," *Fuel*, vol. 89, no. 10, pp. 2651–2664, 2010.

[54] W. Zhu, J. Liu, J. Sheng, and D. Elsworth, "Analysis of coupled gas flow and deformation process with desorption and Klinkenberg effects in coal seams," *International Journal of Rock Mechanics and Mining Sciences*, vol. 44, no. 7, pp. 971–980, 2007.

[55] J. Wang, J. Liu, and A. Kabir, "Combined effects of directional compaction, non-Darcy flow and anisotropic swelling on coal seam gas extraction," *International Journal of Coal Geology*, vol. 109-110, pp. 1–14, 2013.

[56] S. Kong, Y. Cheng, T. Ren, and H. Liu, "A sequential approach to control gas for the extraction of multi-gassy coal seams from traditional gas well drainage to mining-induced stress relief," *Applied Energy*, vol. 131, pp. 67–78, 2014.